Hepatic and Renal Histotripsy in an Anticoagulated Porcine Model

Scott C. Mauch, MD[1], **Annie M. Zlevor, BA**[1], **Emily A. Knott, BS**[1], **Allison B. Couillard, MD**[1], **Sarvesh Periyasamy, BS**[1], **Eliot C. Williams, MD**[2], **John F. Swietlik, MD**[1], **Paul F. Laeseke, PhD, MD**[1], **Xiaofei Zhang, MD**[3], **Zhen Xu, PhD**[4], **E. Jason Abel, MD**[1,5], **Fred T. Lee Jr., MD**[1,5,6], **Timothy J. Ziemlewicz, MD**[1]

[1]Department of Radiology, University of Wisconsin

[2]Department of Medicine, University of Wisconsin

[3]Department of Pathology, University of Wisconsin

[4]Department of Biomedical Engineering, University of Michigan

[5]Department of Urology, University of Wisconsin

[6]Department of Biomedical Engineering, University of Wisconsin

Abstract

Purpose: To determine the risk of mechanical vessel wall damage resulting in hemorrhage during and after hepatic and renal histotripsy in an anticoagulated *in vivo* porcine model.

Materials and Methods: Non-tumor-bearing pigs (n=8, mean weight=52.5kg) were anticoagulated with warfarin (initial dose 0.08 mg/kg) to a target PT of 30-50% above baseline. A total of 15 histotripsy procedures were performed (kidney n=8, 2.0 cm sphere; liver n=7, 2.5 cm sphere). Treatments were immediately followed by CT imaging. Animals were observed for 7 days while continuing anticoagulation, followed by repeat CT and necropsy.

Results: All animals survived to complete the entire protocol with no signs of disability or distress. Three animals had hematuria (pink urine without clots). Baseline prothrombin time (PT) values (mean 16.0 sec) were elevated to 22.0 sec (37.5% above baseline, *p*=0.003) on the day of treatment, and 28.8 sec (77.8% above baseline, *p*<0.001) on the day of necropsy. At the time of treatment 63% (5/8) of subjects were at a therapeutic anticoagulation level, and 100% (8/8) reached therapeutic levels by the time of necropsy. There were no cases of intra-parenchymal,

peritoneal, or retroperitoneal hemorrhage associated with any treatments despite 71% (5/7) of liver and 100% (8/8) of kidney treatments extending to the organ surface.

Conclusion: Liver and kidney histotripsy appears safe with no elevated bleeding risk in this anticoagulated animal model supporting the possibility of histotripsy treatments in patients on anti-coagulation.

INTRODUCTION

Percutaneous thermal ablation confers competing risks of hemorrhage and thrombosis secondary to mechanical and thermal trauma, particularly for anticoagulated patients. Clinically significant hemorrhage and/or hematoma are reported in up to 5% of renal cryoablation patients (1) and up to 4% in liver microwave ablation patients (2). While the risk of hemorrhage is procedure-specific, withholding anticoagulation in the peri-procedural period can result in complications such as stroke, deep venous thrombosis, pulmonary embolus, or myocardial infarction (3). An important but unfulfilled promise of non-invasive focal cancer therapies is that treatments would not require cessation of anticoagulation, potentially decreasing the risk, complexity, and cost of treating cancer patients.

Histotripsy is a non-invasive, non-thermal, non-ionizing, focused ultrasound treatment modality being investigated for human clinical use (4). In contrast to heat-based ablation modalities, including radiofrequency/microwave ablation and high intensity focused ultrasound (HIFU), that destroy tissue through coagulation resulting in a cautery effect, histotripsy relies on a mechanical process called cavitation, caused by the rapid expansion and collapse of endogenous gas bubbles. In contrast to HIFU that uses continuous or long bursts of ultrasound at high duty cycle to heat tissue, histotripsy uses high amplitude, low duty-cycle ultrasound pulses to create cavitation at the focal zone (4). The resultant high local mechanical strain destroys tissue at the cellular and subcellular level. Histotripsy creates precise tissue destruction within the liver and kidney, appears to have salutatory immune-stimulatory effects, and exhibits some degree of tissue selectively, specifically sparing heavily collagenous structures, which may be beneficial when treating near critical structures such as bile ducts, the renal collecting system, and vascular walls (4-6). Prior in vivo animal studies suggest that cavitation may cause local thrombosis by damaging the endothelial layer of vessels, exposing the subendothelium, a powerful stimulant of thrombosis (7,8). However, whether the focal mechanical trauma created by histotripsy damages the integrity of vessel walls and provokes hemorrhage in the presence of anticoagulation is not known.

If histotripsy results in no significant bleeding in an anticoagulated animal model, future research on the treatment of anticoagulated human patients may be warranted. Swine is a long-standing model for evaluation of thrombosis during ablation and has been used to study the efficacy of numerous anticoagulation agents, including warfarin (9,10). The purpose of this study is to determine the risk of hemorrhage during and after hepatic and renal histotripsy in an anticoagulated, human-scale porcine model.

MATERIALS AND METHODS

Experimental Design (Figure 1)

This study was approved by the Institutional Animal Care and Use Committee. Eight healthy female pigs (Yorkshire swine, mean weight 52.5 kg (range 51-55 kg), Arlington, WI) were anticoagulated using oral warfarin, initially dosed daily with 0.08 mg/kg based on prior reports (11). Subjects were monitored daily for evidence of bleeding, including hematuria or melena, changes in behavior, or visible bruising. Blood samples were obtained 5 days before treatment, day of treatment, and after 7 days of observation before necropsy. Following a 5 day warfarin loading period, subjects underwent histotripsy treatments of the liver and kidney followed by an immediate post-procedure cone-beam CT (CBCT) on day of treatment. One subject had an inadequate hepatic sonographic window and therefore received renal treatment only. Subjects were survived for a 7-day observation period during which anticoagulation was continued, and then underwent a second CBCT, euthanasia (intravenous (IV) Beuthanasia-D; Schering-Plough, Kenilworth, NJ), and necropsy. A 7-day follow-up period was utilized after consultation with animal care staff as adequate for evaluation of hemorrhagic complications while balancing animal safety and welfare. The primary endpoint of the study was to evaluate for clinically significant post-procedural bleeding. Secondary endpoints included treatment zone size, pathological evaluation of the treatment zone to elucidate potential mechanisms of thrombosis, presence of vessel thrombosis, pseudoaneurysm formation, biliary dilation, damage to nearby organs (such as bowel), and presence of urine leak.

Blood samples

Samples were assayed for prothrombin time (PT) and a complete blood count (CBC) including hemoglobin, hematocrit, and platelets (IDEXX Laboratories, Westbrook, ME). Adjustments to the warfarin dose were made within the range of 0.04 – 0.08 mg/kg as needed during the subsequent survival period (11). Because there is no validated INR value for pigs, prothrombin time of 30-50% above baseline was targeted as this is considered equivalent to the therapeutic range in humans, while values >50% above baseline are considered equivalent to the human supratherapeutic range (11).

Histotripsy Treatments

On the day of treatment, animals were sedated using IM tiletamine/zolazepam (Telazol; Zoetis, Kalamazoo, MI) and xylazine (AnaSed, Shenandoah, IA), intubated, maintained using inhaled isoflurane gas (1.5-2.5%, Halocarbon Laboratories, River Edge, NJ), and an IV placed. Histotripsy of the liver and kidney was performed according to previously described methods (5,6,12,13). Two spherical treatments were targeted in each animal: 2.5 cm for the liver and 2.0 cm for the right kidney. Renal treatments were in the mid to inferior pole due to sonographic window. All treatments were performed using a prototype therapy system (Histosonics, Inc., Ann Arbor, MI) consisting of a dedicated 1 MHz therapeutic signal generator (active aperture 4.6 x 7.1 cm, focal length 6.0 cm, and a working distance of 4.6 cm), as well as a co-axially aligned 3 MHz phased array diagnostic ultrasound probe (Model C5-2; Analogic Corp, Peabody, MA) for concurrent B-mode visualization of

the target (Figure 2). Proprietary software was used to guide the therapy transducer and prescribe the planned treatment size, shape, and volume.

Computed Tomography (CT) Imaging

Cone-beam CT images (Artis Zee, Siemens Healthineers, Forscheim, Germany) without and with intravenous contrast were obtained immediately post-histotripsy on the day of treatment and after a seven day observation period before necropsy. Parameters included: 12-second rotation, 0.47 mm spatial resolution (isotropic), 24 x 24 x 17 cm FoV, Iohexol 300 mg/mL at 2 ml/kg (Omnipaque 300, GE Medical, Waukesha, WI), 3 mL/s with a 45 second delay for imaging of the liver, and approximately 5 minute delayed images for the renal collecting system.

Imaging Analysis

CT images were analyzed on an institutional PACS (McKesson, San Francisco, CA) by a radiology resident (PGY-4) and a faculty radiologist (10 years of ablation experience) in consensus, and assessed for intra- or extra-peritoneal blood, active bleeding, hematoma, pseudoaneurysm, thrombus, and off-target injury for the liver and kidney. Additionally delayed images were utilized to evaluate for urine leak, urinary system clot or debris, and hydronephrosis.

Histopathology

Focused necropsy was completed following euthanasia. The body wall, abdominal, and thoracic cavities were inspected for any evidence of bleeding as well as off-target treatment effects. Targeted lobes of the liver and the right kidney were removed, photographed, and fixed in 10% buffered formalin. Treatment zones were sectioned and placed in cassettes. Samples were then processed in a Sakura Tissue-Tek VIP (Sakura Finetek, Torrance, CA) and embedded with a Leica EG 1160 (Leica Biosystems, Richmond, IL). Five micron-thick sections were cut using a Leica RM2125RT (Leica Biosystems, Richmond, IL) and stained with hematoxylin and eosin. Selected blocks were stained with Masson's trichrome and Verhoeff's Van Geison/EVG stain to highlight collagen and elastic fibers. A pathologist with 8 years of clinical experience then evaluated the samples.

Statistical Analysis

The sample size was based on standards from prior animal studies and in consultation with veterinary animal care experts. Two-sided t-tests were used to compare the prescribed and actual measurements of the volume and anterior-posterior, medial-lateral, and cranial-caudal dimensions of the treatments. Lab values at each time point were summarized by the median and inter-quartile range (IQR) and were compared between baseline, treatment, and necropsy using box plots and the Kruskal-Wallis (or Wilcoxon rank sum) tests. A p-value less than 0.05 was considered statistically significant. All statistical analyses were performed using R (Version 4.0.2; R Foundation for Statistical Computing, Vienna, Austria).

RESULTS

No clinically significant bleeding events occurred in the follow-up period and there was no death, disability, change in behavior, or sign of distress during or after treatment. Notably, treatment zones extended to the liver capsule in five cases with no evidence of subcapsular or peritoneal hematoma at imaging or necropsy (Figure E1). In one case, the treatment extended through the liver capsule and into the adjacent spleen without hemorrhage (Figure 3). In the kidney, all 8 treatment zones extended to the capsule. Two small perirenal fluid collections (1.9 x 2.2 cm and 1.5 x 3.5 cm) noted on imaging the day of the treatment resolved by Day 7 (Figure 4A, E2). Two of the subjects had minimal urine leaks into treatment zones on the day of necropsy (Figure 4B) without urinomas or extravasation. No significant hemorrhage was noted in the peri-renal space or the collecting system at imaging or necropsy. Transient hematuria with pink urine (but no bright red blood or clots) was seen in 38% (3/8) of animals and resolved within three days. Two of the three hematuria animals were housed together, and hematuria could not be attributed to a single animal so was assigned to both. There were 4 cases of lobar portal vein thrombus, 3 of which resolved by day 7 (75%). A summary of imaging findings is in Table 1.

Warfarin dosing and PT

All animals were started on a dose of 0.08 mg/kg warfarin 5 days before treatment. Another PT was drawn immediately preceding treatment, and the dose was subsequently adjusted in 6/8 based on the results (Table 2—four increased and two decreased). By day of treatment, 63% (5/8) of animals had achieved either a therapeutic (>30 to <50% above baseline) or supratherapeutic (50% above baseline) level of anticoagulation with a mean increase in PT from baseline of 37.5% (p=0.003 vs. baseline). By day of necropsy, 100% (8/8) animals had achieved at least therapeutic levels (75% or 6/8 supra-therapeutic) with a mean increase in PT of 77.8% above baseline (p<0.001).

Complete Blood Count

Pertinent CBC and PT results are displayed in Figure 5 with all results in Table E1. Of note, mean hemoglobin 5 days before treatment was 13.4 g/dL and had decreased to 11.8 g/dL by day of treatment, even before treatment occurred (p=0.001). After 7 days of observation following the treatment, mean hemoglobin had decreased to 10.7 g/dL with the largest individual decrease of 1.9 g/dl (p=0.08).

Treatment Zone

Liver—The mean hepatic ablation zone was slightly larger than the prescribed size (prescribed diameter=2.5 cm spherical), mean actual diameter=3.2 cm, p=0.02. Between the day of treatment and necropsy, there was a slight decrease in mean treatment zone size (3.0 to 2.8 cm).

Kidney—The mean ablation zone on imaging was slightly larger than prescribed, particularly in the CC dimension (prescribed diameter=2.0 cm spherical, mean actual diameter=2.4 cm, mean CC dimension=2.6 cm, p0.003 for prescribed vs. actual in transverse and CC) and all extended to the kidney surface.

Histopathology

Liver—Complete cell death was present within the treatment zone in all cases with a narrow zone of transition between ablated and normal liver. Within the treatment zone there were three distinct patterns of cell death: 1) An acellular pattern (n=3, Figure 6A) consisting of a featureless acellular homogenate with interspersed red blood cells and fibrinous clot. Rare fragments of cellular debris were present within the homogenate, and all supporting elements of hepatic lobules (vessels, bile ducts, fibrous tissue) were destroyed, 2) Ischemic pattern (n=1, Figure 6B) was characterized by selective destruction of hepatocytes with retention of the overall hepatocellular contour and lobular hepatic architecture including blood vessels and portal tracts, 3) Mixed-pattern (n=3, Figure 6C) was characterized by an acellular pattern in the central portions and an ischemic-type pattern at the periphery of the treatment zone. For all three patterns, there was fibroblast proliferation at the rim of the treatment forming a pseudo-capsule. Outside of the treatment zone, there was no evidence of damage to hepatocytes or other hepatic structures.

Kidney—All kidney treatments were predominantly acellular, consisting of cell fragments and red cells without residual viable cells. Similar to the acellular pattern in the liver specimens, there was a narrow transition zone between normal kidney and the treatment zone, a surrounding fibrous pseudocapsule, and no evidence of off-target injury. There was no evidence of an ischemic-type pattern of injury in the kidney.

Vessels and Hemorrhage—In cases in which the acellular pattern predominated, thrombosis and endothelial damage of vessels immediately adjacent to the treatment zone was a prominent feature (Figure 6D, E). In cases in which the ischemic pattern was prominent, there was no evidence of hemorrhage into or surrounding the treatment zone. The vessels in the surrounding border tissues appeared normal without significant endothelial damage or thrombosis.

Capsular integrity—Both acellular and ischemic treatment patterns were noted extending to the liver and kidney capsule. When the capsule was involved, it remained intact with inflammatory cells and sparse hemorrhage interspersed between intact fibroblasts (Figure 6F).

DISCUSSION

The mechanical nature of cavitation has led to fears that histotripsy may damage the integrity of blood vessels within the treatment zone, resulting in uncontrolled hemorrhage (14). However, prior animal studies have demonstrated a lack of bleeding after histotripsy of the liver, prostate, and kidney (5,6,14,15) and the results of this study show that hemorrhage does not occur even in anticoagulated animals with ablations extending to and through the organ surface. Four subjects were noted to develop portal vein thrombus (transient in 75% or 3/4 subjects), which is consistent with results of prior studies examining histotripsy treatments within the liver (5).

To date, little is known about the use of histotripsy in the setting of therapeutic anticoagulation. Histotripsy in anticoagulated dog prostate (14) and heparinized pig liver

did not demonstrate bleeding, but animals were neither survived nor imaged (15). Another non-invasive ablation method, HIFU, has shown no hemorrhage when treating thyroid and muscle in anti-coagulate models, though depends on coagulation for tissue death and thus would be expected to have lower bleeding risk (16,17). There have been no studies examining the effects of HIFU combined with anticoagulation in liver or kidney.

Current SIR guidelines classify invasive procedures to diagnose and treat disease in the liver and kidney as high risk for bleeding and recommend correcting INR to a range of   1.5-1.8 if elevated above this level. In patients with chronic liver disease the cut-off changes to INR <2.5 given the complexity of the underlying coagulation state (18). This is balanced with patient risk for complications from thrombosis and bridging with low-molecular weight heparin should be considered. If findings from this study can be replicated in humans, the need to take patients off warfarin and bridge would be negated thus decreasing patient care complexity and risk.

The histopathologic findings in this study help explain the apparent contradiction of mechanical vascular damage that does not result in bleeding, even in the extreme case of supratherapeutic anticoagulation. In subjects with an acellular pattern, small vessels in the central portions of the ablation zone were obliterated, and vessels on the periphery were found to have endothelial damage causing thrombosis. By one week there was formation of a nascent fibrous pseudocapsule and the capsule remained intact, even when the treatment extended to the organ surface. There was no evidence of more brisk or extensive bleeding by imaging or at necropsy. In livers with an ischemic-type response, vessels and hepatic architecture remained intact (even in the central ablation zone), and thus there was no mechanism for bleeding. Therefore, regardless of whether the acellular or ischemic pattern predominated after histotripsy, bleeding did not occur in the immediate post-procedure period, and the risk of delayed hemorrhage appears low.

The choice of model in this study was multifactorial. The normal swine model used in this study is a standard animal model for testing percutaneous ablation devices (5,6,19) and has been used as a translational model for histotripsy (5,6,12,13). Warfarin was the only anticoagulant used in this study due to prior use in pigs and known levels of species-specific therapeutic anticoagulation (14,16,17). Newer direct oral anticoagulants (DOACs) are becoming increasingly popular due to a simple dosing schedule and lack of need for periodic laboratory monitoring. However, confirmation of therapeutic ranges with DOACs requires custom validation not readily available in animals. Given that prior RCT and registry studies demonstrated similar or lower post-procedural bleeding rates for DOACs compared to warfarin (3,20-24), the results of this support exploring subjects undergoing histotripsy while on DOACs. While international normalized ratio (INR) is traditionally used to monitor the effects of warfarin in humans, there is no validated INR standard in pigs. Therefore, PT was used in this study based on reference PT values from prior animal studies (11).

The frequency and timing of blood draws and warfarin dose adjustments merits discussion. Venous blood sampling in pigs is traumatic and requires either anesthesia or specialized restraint equipment not available at our facility. To minimize animal distress, PT was

assessed when general anesthesia was otherwise planned, resulting in only five of eight (63%) subjects in the therapeutic or supra-therapeutic range of PT on the day of treatment. However, two of the three subjects that were not therapeutic at the time of treatment had PT values substantially higher than baseline and all three had their warfarin dose increased to the maximum recommended dose. Moreover, all 8 animals, including the three that were initially subtherapeutic, were either therapeutic or supratherapeutic on the day of necropsy. Importantly, no significant bleeding was detected in any animal at any timepoint regardless of level of anticoagulation. This includes those that were supratherapeutic either at the time of the procedure or in follow-up.

This study has limitations, including that urinalysis was not performed due to a need for anesthesia for collection, a small sample size, and lack of a control group. Additionally, the risk of bleeding when targeting major vessels was not evaluated as the treatment zones were targeted to parenchyma to mimic common location of solid organ tumors. Future research could evaluate the risk of bleeding when treatment zones directly target vessels. The study was also limited due to the evaluation of only one type of anticoagulation agent in one specific clinical scenario. As such, the results of the study may not apply to all agents or coagulation states. Finally, the sample size was determined by standard from similar experiments rather than power calculation, limiting the statistical validity.

In summary, the results of this study suggest that liver and kidney histotripsy may be safe in an anticoagulated animal model, even when the ablations extend through the organ capsule, and a mechanism for post-histotripsy hemostasis is proposed based on histologic findings. Further research is suggested to evaluate histotripsy in the setting of other forms of anticoagulation, cirrhotic and/or tumored models, and eventually in human subjects.

Supplementary Material

Refer to Web version on PubMed Central for supplementary material.

Acknowledgements:

References

1. Atwell TD, Carter RE, Schmit GD, et al. Complications following 573 Percutaneous Renal Radiofrequency and Cryoablation Procedures. Journal of Vascular and Interventional Radiology. 2012;23(1):48–54. doi:10.1016/j.jvir.2011.09.008 [PubMed: 22037491]

2. Facciorusso A, Abd El Aziz MA, Tartaglia N, et al. Microwave Ablation Versus Radiofrequency Ablation for Treatment of Hepatocellular Carcinoma: A Meta-Analysis of Randomized Controlled Trials. Cancers (Basel). 2020;12(12):3796. doi:10.3390/cancers12123796 [PubMed: 33339274]

3. Spyropoulos AC, Al-Badri A, Sherwood MW, Douketis JD. Periprocedural management of patients receiving a vitamin K antagonist or a direct oral anticoagulant requiring an elective procedure

or surgery. Journal of Thrombosis and Haemostasis. 2016;14(5):875–885. doi:10.1111/jth.13305 [PubMed: 26988871]

4. Xu Z, Hall TL, Vlaisavljevich E, Lee FT. Histotripsy: the first noninvasive, non-ionizing, non-thermal ablation technique based on ultrasound. International Journal of Hyperthermia. 2021;38(1):561–575. doi:10.1080/02656736.2021.1905189 [PubMed: 33827375]

5. Smolock AR, Cristescu MM, Vlaisavljevich E, et al. Robotically assisted sonic therapy as a noninvasive nonthermal ablation modality: Proof of concept in a porcine liver model. Radiology. 2018;287(2):485–493. doi:10.1148/radiol.2018171544 [PubMed: 29381870]

6. Knott EA, Swietlik JF, Longo KC, et al. Robotically-Assisted Sonic Therapy for Renal Ablation in a Live Porcine Model: Initial Preclinical Results. Journal of Vascular and Interventional Radiology. 2019;30(8):1293–1302. doi:10.1016/j.jvir.2019.01.023 [PubMed: 31130365]

7. Shen ZY, Liu C, Wu MF, et al. Spiral computed tomography evaluation of rabbit VX2 hepatic tumors treated with 20 kHz ultrasound and microbubbles. Oncology Letters. 2017;14(3):3124–3130. doi:10.3892/ol.2017.6557 [PubMed: 28928850]

8. Delius M, Denk R, Berding C, et al. Biological effects of shock waves: Cavitation by shock waves in piglet liver. Ultrasound in Medicine & Biology. 1990;16(5). doi:10.1016/0301-5629(90)90169-D

9. Lester PA, Coleman DM, Diaz JA, et al. Apixaban Versus Warfarin for Mechanical Heart Valve Thromboprophylaxis in a Swine Aortic Heterotopic Valve Model. Arterioscler Thromb Vasc Biol. 2017;37(5):942–948. doi:10.1161/ATVBAHA.116.308649 [PubMed: 28232327]

10. Ke L, Ni H bin, Tong Z hui, et al. Efficacy of continuous regional arterial infusion with low-molecular-weight heparin for severe acute pancreatitis in a porcine model. Shock. 2014;41(5):443–448. doi:10.1097/SHK.0000000000000129 [PubMed: 24430546]

11. Cromeens DM, Rodgers GP, Minor ST. Warfarin sodium for anticoagulation of atherosclerotic miniature swine. J Invest Surg. 1990;3(2). doi:10.3109/08941939009140344

12. Longo KC, Knott EA, Watson RF, et al. Robotically Assisted Sonic Therapy (RAST) for Noninvasive Hepatic Ablation in a Porcine Model: Mitigation of Body Wall Damage with a Modified Pulse Sequence. CardioVascular and Interventional Radiology. 2019;42(7):1016–1023. doi:10.1007/s00270-019-02215-8 [PubMed: 31041527]

13. Longo KC, Zlevor AM, Laeseke PF, et al. Histotripsy Ablations in a Porcine Liver Model: Feasibility of Respiratory Motion Compensation by Alteration of the Ablation Zone Prescription Shape. CardioVascular and Interventional Radiology. 2020;43(11):1695–1701. doi:10.1007/s00270-020-02582-7 [PubMed: 32676957]

14. Wheat JC, Hall TL, Hempel CR, et al. Prostate histotripsy in an anticoagulated model. Urology. 2010;75(1). doi:10.1016/j.urology.2009.09.021

15. Vlaisavljevich E, Owens G, Lundt J, et al. Non-Invasive Liver Ablation Using Histotripsy: Preclinical Safety Study in an In Vivo Porcine Model. Ultrasound Med Biol. 2017;43(6). doi:10.1016/j.ultrasmedbio.2017.01.016

16. Lang BH, Woo YC, Chiu KWH. High intensity focused ultrasound (HIFU) ablation of benign thyroid nodule is safe and efficacious in patients who continue taking an anti-coagulation or anti-platelet agent in the treatment period. Int J Hyperthermia. 2019;36(1). doi:10.1080/02656736.2018.1548034

17. Kaye EA, Solomon SB, Gutta NB, et al. High-intensity focused ultrasound ablation of muscle in an anticoagulated swine model. Minim Invasive Ther Allied Technol. Published online June 3, 2020:1–5. doi:10.1080/13645706.2020.1760301

18. Patel IJ, Rahim S, Davidson JC, et al. Society of Interventional Radiology Consensus Guidelines for the Periprocedural Management of Thrombotic and Bleeding Risk in Patients Undergoing Percutaneous Image-Guided Interventions—Part II: Recommendations. Journal of Vascular and Interventional Radiology. 2019;30(8):1168–1184.e1. doi:10.1016/j.jvir.2019.04.017 [PubMed: 31229333]

19. Cornelis FH, Durack JC, Kimm SY, et al. A Comparative Study of Ablation Boundary Sharpness After Percutaneous Radiofrequency, Cryo-, Microwave, and Irreversible Electroporation Ablation in Normal Swine Liver and Kidneys. Cardiovasc Intervent Radiol. 2017;40(10). doi:10.1007/s00270-017-1692-3

20. Nagata N, Yasunaga H, Matsui H, et al. Therapeutic endoscopy-related GI bleeding and thromboembolic events in patients using warfarin or direct oral anticoagulants: results from a large nationwide database analysis. Gut. 2018;67(10). doi:10.1136/gutjnl-2017-313999

21. Yagyuu T, Kawakami M, Ueyama Y, et al. Risks of postextraction bleeding after receiving direct oral anticoagulants or warfarin: a retrospective cohort study. BMJ Open. 2017;7(8). doi:10.1136/bmjopen-2017-015952

22. Yanagisawa N, Nagata N, Watanabe K, et al. Post-polypectomy bleeding and thromboembolism risks associated with warfarin vs direct oral anticoagulants. World Journal of Gastroenterology. 2018;24(14). doi:10.3748/wjg.v24.i14.1540

23. Essebag V, Healey JS, Joza J, et al. Effect of Direct Oral Anticoagulants, Warfarin, and Antiplatelet Agents on Risk of Device Pocket Hematoma: Combined Analysis of BRUISE CONTROL 1 and 2. Circ Arrhythm Electrophysiol. 2019;12(10). doi:10.1161/CIRCEP.119.007545

24. Palareti G. Direct oral anticoagulants and bleeding risk (in comparison to vitamin K antagonists and heparins), and the treatment of bleeding. Semin Hematol. 2014;51(2). doi:10.1053/j.seminhematol.2014.02.002
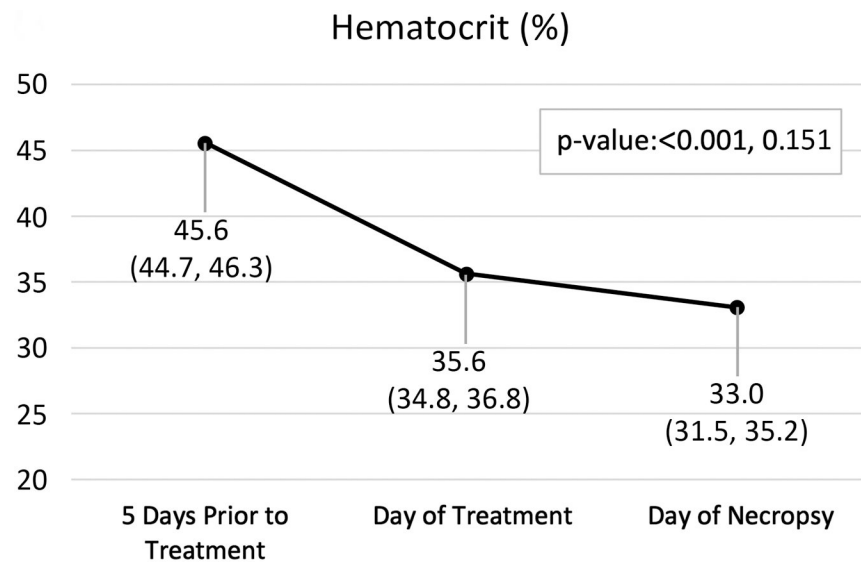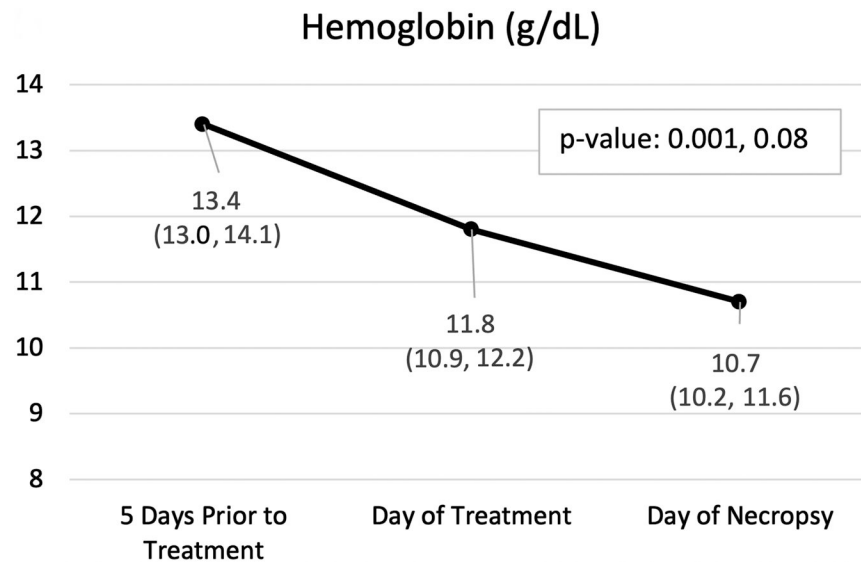
Author Manuscript

Author Manuscript

Author Manuscript
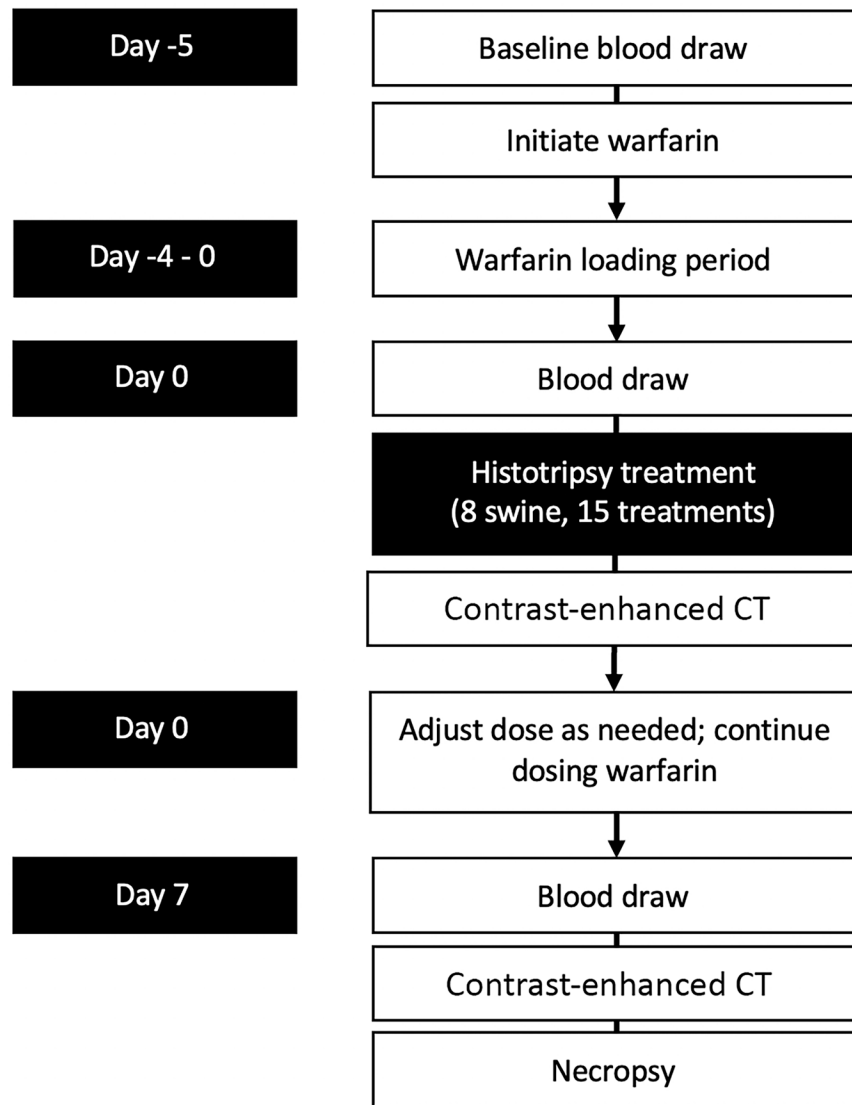
Author Manuscript

Figure 1.
Experimental design
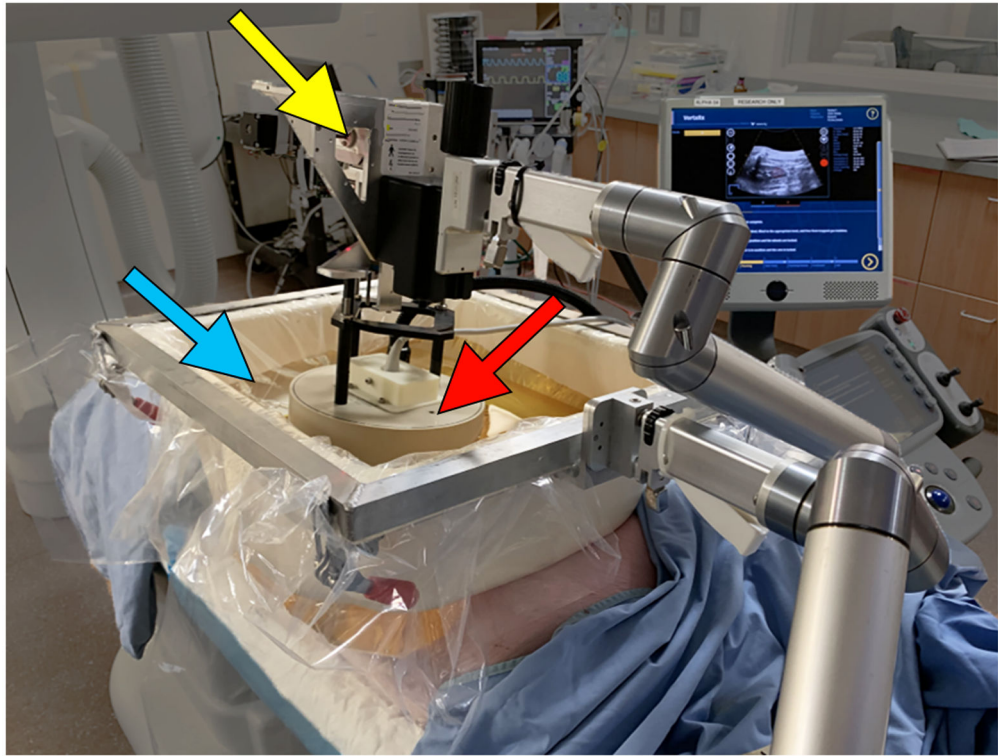
Figure 2.
Histotripsy device schematic demonstrating the therapy transducer (red arrow), water bath (blue arrow), and housing unit with micro-positioning motors (yellow arrow).
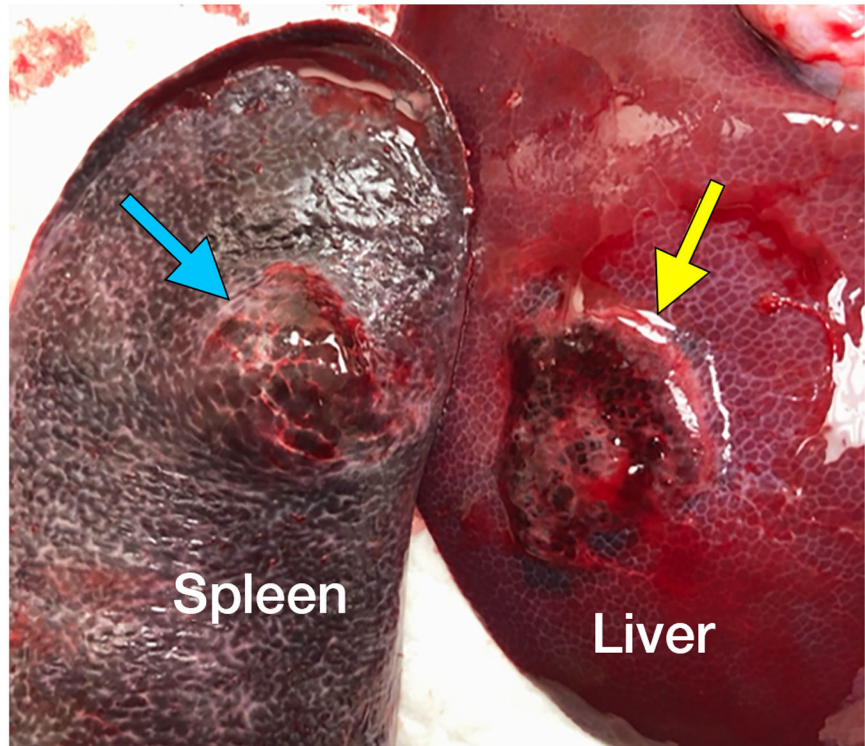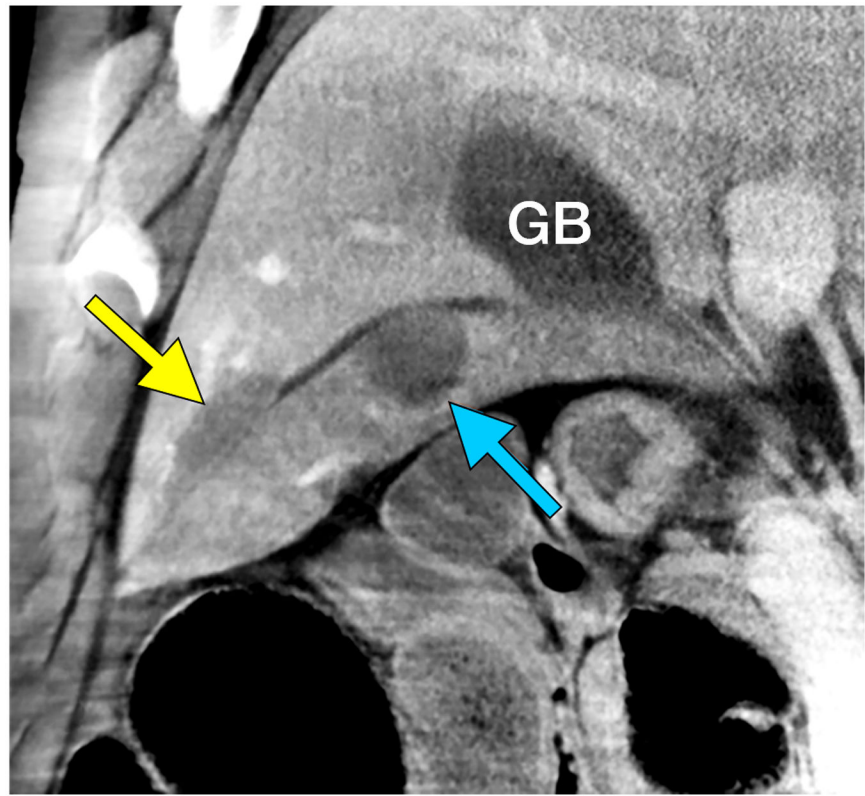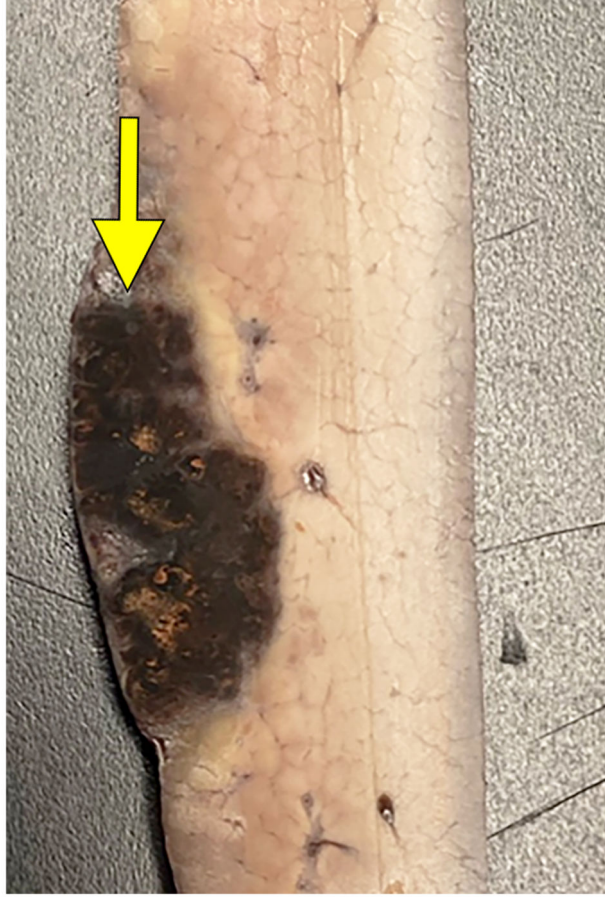
Figure 3.
Extension of the ablation zone from the liver (yellow arrow) into the spleen (blue arrow)
without causing bleeding. CT image demonstrates hepatic ablation zone extending into
spleen (A). The gallbladder (GB) is seen medial to the splenic ablation site. The lack
of proximity of the hepatic and splenic ablation sites is due to free movement of the
porcine spleen during the seven days between treatment and scanning. (B) Dissection image
demonstrates extension of the ablation zone from the liver (3.0 cm) to the spleen (2.8 cm)
without intervening hematoma. (C) Cross section of the liver surface showing ablation zone
(2.0 cm).
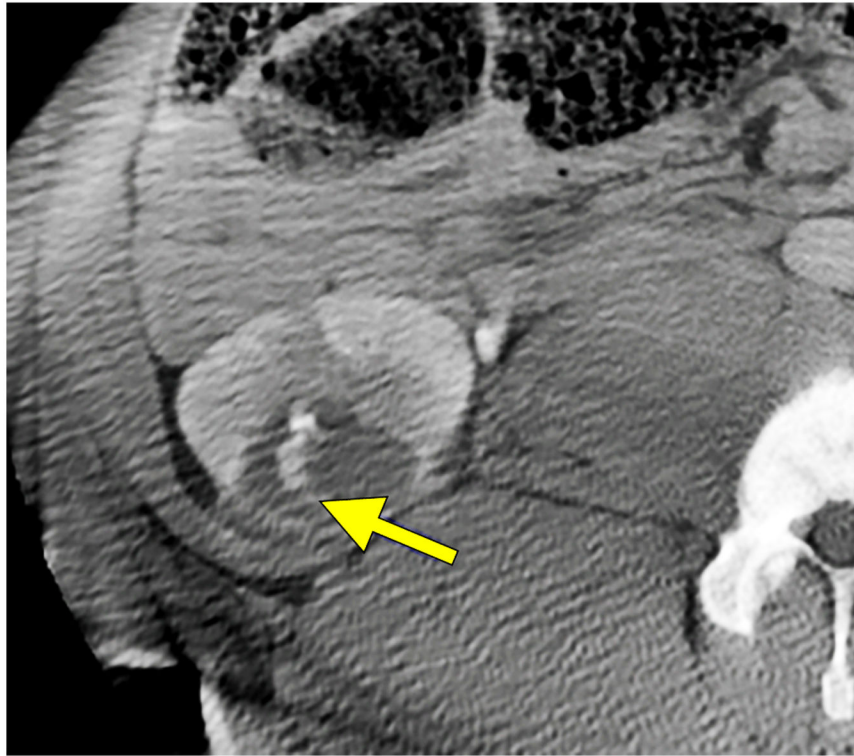
Figure 4.
Small peri-renal fluid collection with near-resolution. Reconstructed coronal images immediately post treatment (A) demonstrate a small peri-renal collection of fluid density (red arrows) at the inferior pole of the kidney adjacent to the treatment zone measuring 1.5 x 3.5 cm on treatment day. Example of a small urine leak (yellow arrow) into treatment zone on post-procedure day 7 on axial CT images (B).

Hemoglobin (g/dL)

p-value: 0.001, 0.08

13.4
(13.0, 14.1)

11.8
(10.9, 12.2)

10.7
(10.2, 11.6)

5 Days Prior to Treatment   Day of Treatment   Day of Necropsy

Hematocrit (%)

p-value:<0.001, 0.151

45.6
(44.7, 46.3)

35.6
(34.8, 36.8)

33.0
(31.5, 35.2)

5 Days Prior to Treatment   Day of Treatment   Day of Necropsy

Prothrombin time (sec)

15.6
(15.3, 17.0)

21.9
(18.1, 25.0)

25.7
(23.2, 30.0)

p-value: 0.003, 0.109

5 Days Prior to Treatment · Day of Treatment · Day of Necropsy
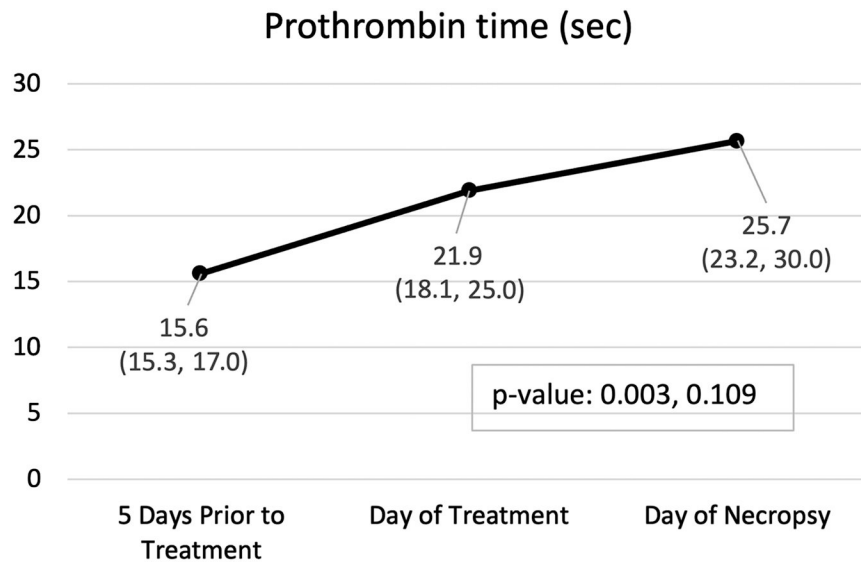
Figure 5:
Hemoglobin (**A**), hematocrit (**B**), and prothrombin time (**C**) by time point. Variables are summarized by median (inter-quartile range); p-values are based on the Wilcoxon rank sum test (Base v. Treat, Treat v. Necropsy).
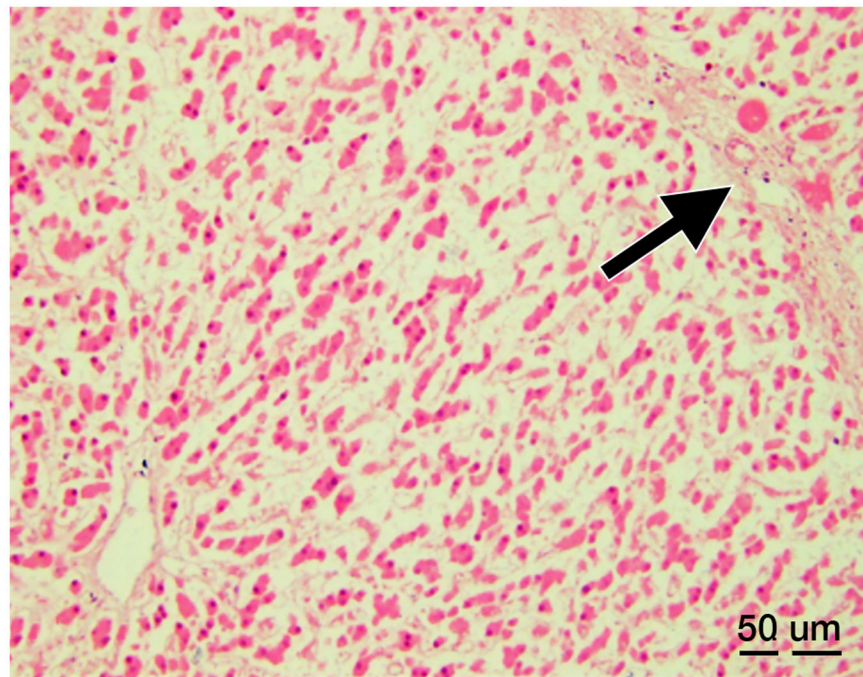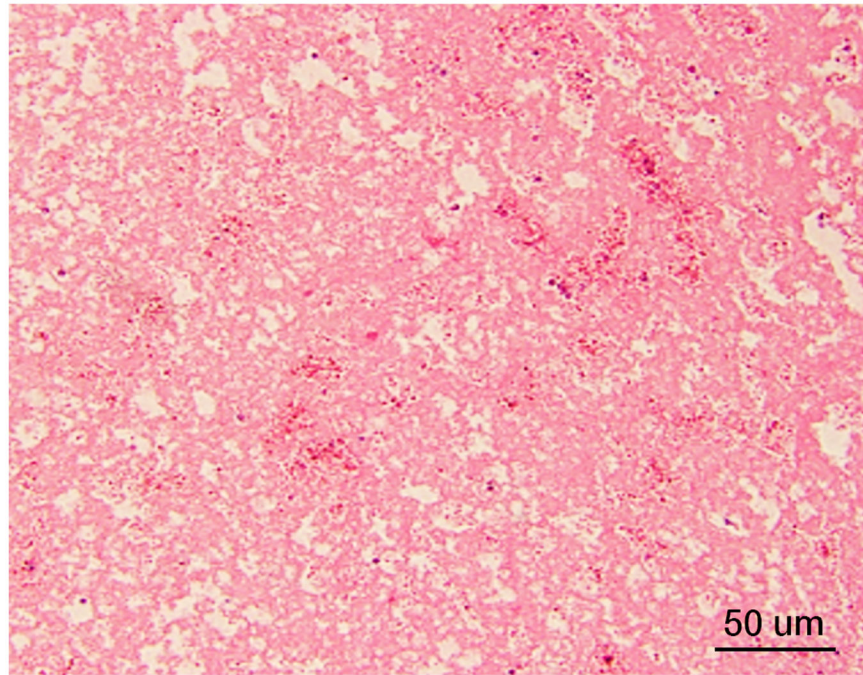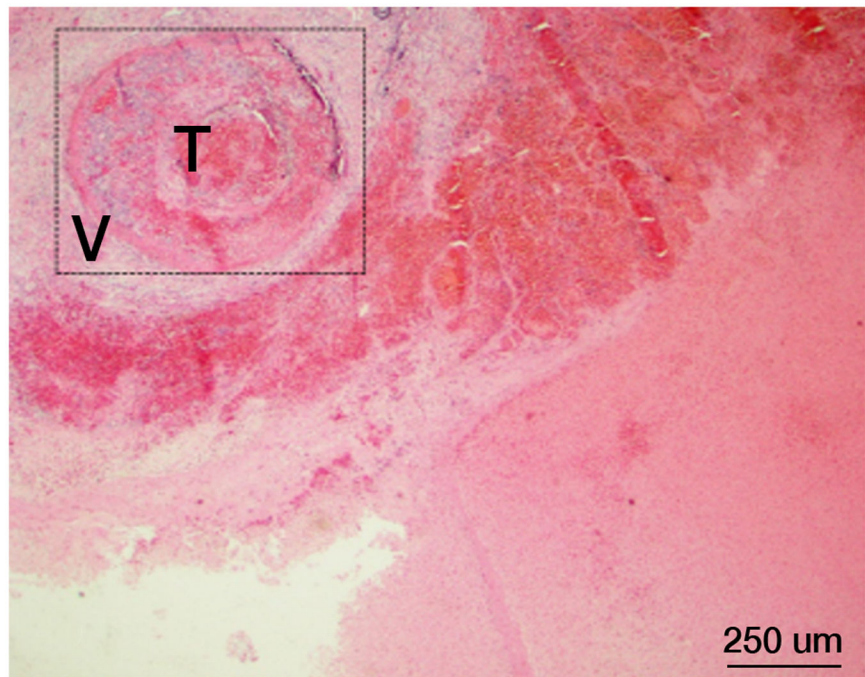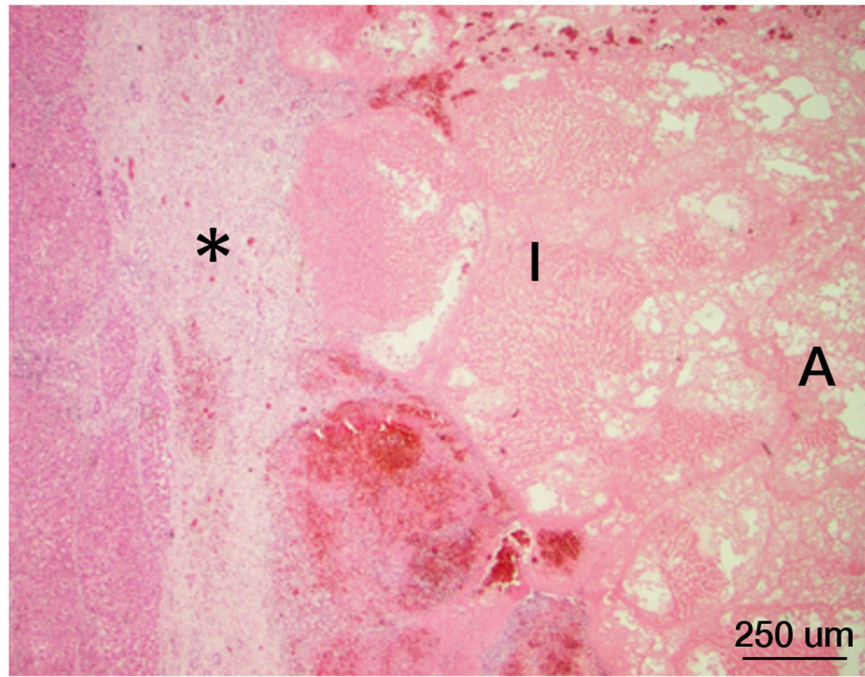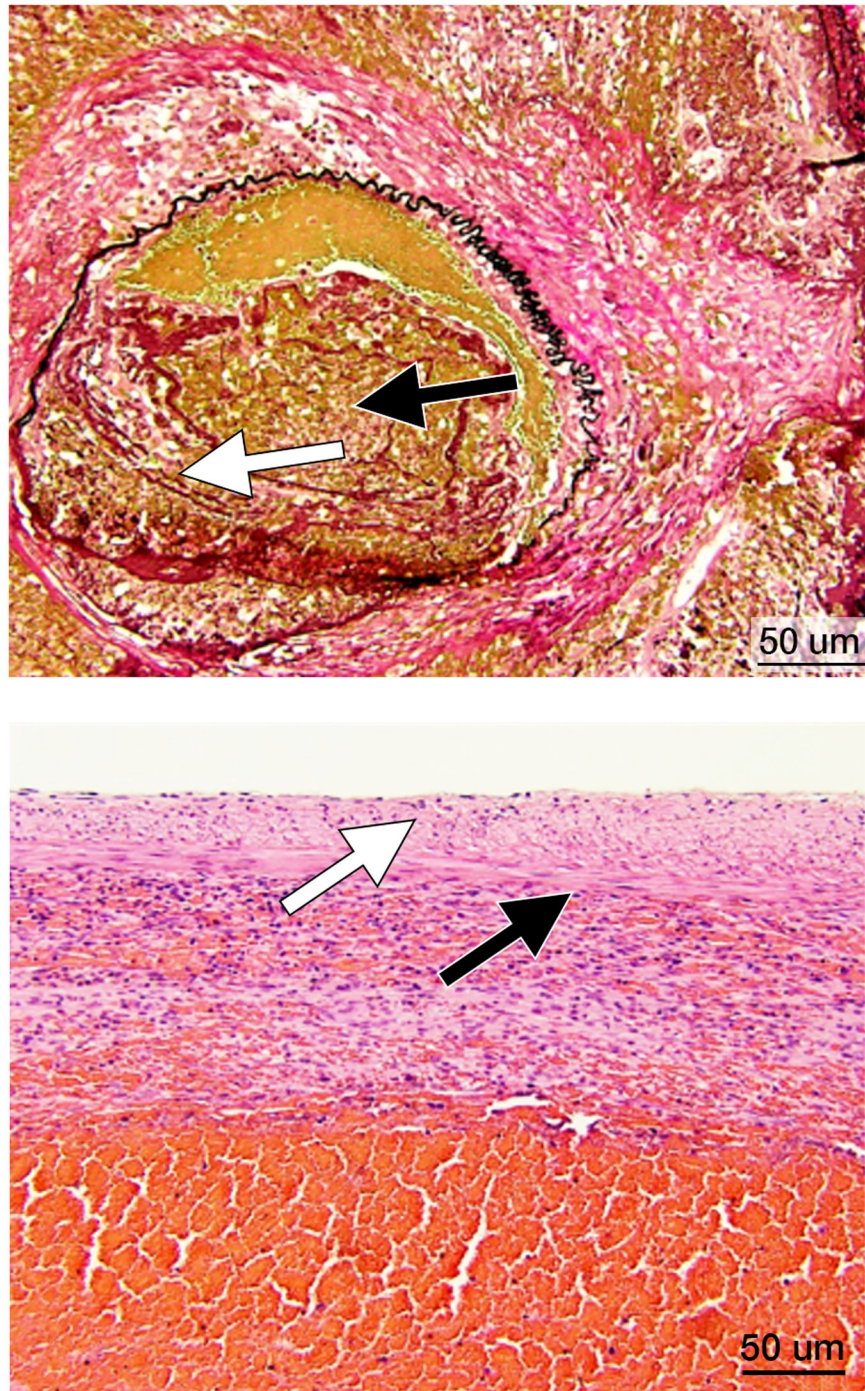
Figure 6.
Histopathology after histotripsy. **A)** The acellular pattern, with featureless blood and fibrin clot mixed with red blood cells, and no residual hepatic architecture. In this pattern, small blood vessels and portal triads are obliterated. (Magnification: 10X. Scale bar: 50μm). **B)** The ischemic pattern, with completely necrotic hepatocytes but preserved collagenous architecture including the framework of portal triads. Note the trabecular architecture and portal tract (black arrow) in the upper right. The contour of bile duct, portal vein and hepatic

artery within the portal triad can still be recognized. (Magnification: 10X. Scale bar: 50μm). **C)** The Mixed pattern. Note the acellular pattern in the center of the ablation zone (A, Right) and the ischemic pattern at the ablation periphery (I, center). Also note the fibroblastic proliferation forming a "pseudo-capsule" (*) at the rim of the ablation zone. (Magnification: 2X. Scale bar: 250μm). **D)** Vascular injury. In this case, there is a thrombosed vessel (V) adjacent to the ablation zone. The vessel demonstrates evidence of endothelial injury and complete obstruction by the central thrombus (T) (Magnification: 2X. Scale bar: 250μm). **E)** High power of the Verhoeff Van Gieson/EVG stain of the injured vessel with thrombus. (Magnification: 10X. Scale bar: 50μm). The internal elastic lamina of this medium sized artery is highlighted as black by Verhoeff Van Gieson/EVG stain. Please note the disruption of the internal elastic lamina (white arrow) and the thrombus in the lumen (black arrow). **F)** Intact capsule with a subcapsular ablation zone in the kidney. Note the intact fibrous layer (black arrow) and intact mesothelial lining (white arrow) of the capsule despite extension of the ablation zone immediately adjacent to the capsule. (Magnification: 10X. Scale bar: 50μm).

Table 1.

Summary of CT findings after liver and kidney histotripsy treatments

	Day of Treatment	Day of Necropsy
Liver (n = 7)		
Extension to organ surface	3	2
Extravasation	0	0
Injury to bowel or abdominal wall	0	0
Intraparenchymal hematoma	0	0
Retroperitoneal hematoma	0	0
Pseudoaneurysm	0	0
Portal vein thrombus	4	1
Hepatic vein thrombus	0	0
Perfusion defect	5	5
Subcapsular hematoma	0	0
Biliary ductal dilation	0	2
Kidney (n = 8)		
Extension to organ surface	7	7
Intraparenchymal hematoma	0	0
Extravasation	0	0
Injury to bowel or body wall	0	0
Subcapsular hematoma	0	0
Urine leak	0	2
Delayed nephrogram	0	0
Blood in collecting system	3	0
Pseudoaneurysm	0	0

Table 2.

Warfarin dosing and prothrombin values

Subject	Five Days Prior to Treatment		Day of Treatment				Day of Necropsy			
	PT (sec)	Dose (mg/kg)	PT (sec)	PT from baseline	Dose (mg/kg)	Dose from baseline (mg/kg)	PT (sec)	PT from baseline	Dose (mg/kg)	Dose from treatment (mg/kg)
1	15.3	0.08	25.4 **	66.0%	0.04	−0.02	20.7 *	35.3%	0.04	0
2	17.3	0.08	22.5 *	30.1%	0.07	0.01	34.3 **	98.3%	0.07	0
3	15.5	0.08	18.3	18.1%	0.08	0.02	27.2 **	75.5%	0.07	−0.01
4	15.1	0.08	17.4	15.2%	0.08	0.02	22.3 *	47.7%	0.07	−0.01
5	17.0	0.08	16.1	−5.3%	0.08	0.02	28.5 **	67.6%	0.08	0
6	17.1	0.08	24.9 *	45.6%	0.06	0.00	49.6 **	190.1%	0.06	0
7	15.3	0.08	29.8 **	94.8%	0.04	−0.02	23.5 **	53.6%	0.04	0
8	15.7	0.08	21.3 *	35.7%	0.06	0	24.2 **	54.1%	0.06	0
Mean	16.0	0.08	22.0 *	37.5%	0.06	0.00	28.8 **	77.8%	0.06	0.00

PT = prothrombin time

*
indicates the subject was at a therapeutic level of anticoagulation (30-50% PT from baseline)

**
indicates supra-therapeutic level of anticoagulation (>50% PT from baseline)